Progress In Electromagnetics Research, PIER 100, 189–200, 2010

A DUAL-POLARIZED WIDE-BAND PATCH ANTENNA FOR INDOOR MOBILE COMMUNICATION APPLICATIONS

M. Secmen and A. Hizal

Department of Electrical and Electronics Engineering
Middle East Technical University
Ankara, Turkey

Abstract—This paper proposes the configuration of a dual-polarized wide-band patch antenna system suitable for indoor mobile communication applications. This configuration consists of two patch antennas, which have different feed structures from classical patch antenna configuration. These antennas, which are separated by a thin absorber to have a good isolation, are fed independently to obtain dual polarization. The antenna structure is designed, simulated, manufactured and measured. The operation bandwidth spans 1900–2700 MHz covering Bluetooth, Wireless Local Area Networks (WLAN) and Universal Mobile Telecommunications System (UMTS) bands. The simulations show good agreement with the measurement results that the antennas have return losses higher than 15 dB, and the coupling between two antennas is below −20 dB within the operation band.

1. INTRODUCTION

Wireless communication systems have received increased interests in recent years. Especially, cellular phone systems or wireless local area networks (WLANs) have increased due to the increase in the number of people using their services. While these systems basically span the frequency band of 1900–2500 MHz, with the development of new technology of 3G mobile systems, which operates in the band 2500–2700 MHz [1], the total operation bandwidth expands to 1900–2700 MHz for multi-functional operations. In indoor environment, integrated networks serving all operators are commonly installed. For this implementation, wideband or multiband antennas are needed [2].

Corresponding author: M. Secmen (msecmen@eee.metu.edu.tr).

Therefore, the indoor antennas or systems should cover the given frequency bandwidth by satisfying the necessary requirements [3–6]. In addition to this property, the antenna system should maximize the signal-to-noise ratio with respect to polarization. One of the most commonly used techniques to achieve this is the polarization diversity [7, 8], which mainly consists of two antenna elements obtaining two uncorrelated signal components and combining properly at the receiver side. While circular polarization is used for relatively narrower band applications [9], dual polarization is commonly used for most of these applications [1, 10, 11].

This paper introduces a wide-band dual-polarized patch antenna system suitable for indoor mobile communication system applications. The structure, which is also compact (small size), lightweight and relatively cheap, covers the operation frequency bands of wireless local area networks, universal mobile telecommunication systems (UMTS) I and II. The structure mainly consists of two antennas separated by an absorber wall and the antennas are oriented orthogonally with a special feed construction in order to provide dual polarization. The structure is initially fed by classical microstrip lines attached to bottom-mounted probes. Afterwards, these lines are terminated with the transition structures, and small metal plates, "feed elements", at a certain height feeding the patch antennas with coupling mechanism. The "parasitic elements", which are vertical plates connecting the patch antennas and substrate (not the ground plane), also exist in the structure to increase the antenna performance. This structure has been designed, simulated and manufactured. The measurement results are supported with the simulation results, which show high similarities especially in return loss and radiation patterns and the antenna perform satisfactorily with respect to return loss, coupling and radiation pattern within the wide frequency band of 1900–2700 MHz (about 34% bandwidth).

2. THE ANTENNA STRUCTURE

The antenna structure is composed of two identical square thin (0.2 mm) patch antennas above FR4 substrate ($\varepsilon_r = 4.4$, tangent loss = 0.02, thickness = 1.52 mm) fed by a particular microstrip construction and separated by a low-cost absorber material (ECCOSORB® LS-26). The simulation view of whole structure is given in Figure 1. As shown in Figure 1, the structure contains two orthogonal (± 45 degrees) 50 Ω microstrip lines for each polarization port at the input side fed by bottom-mounted probes (not given in Figure 1 for the simplicity). Subsequently, input power is transferred to the feed elements via bow-tie transitions, which feed the patch antennas for the radiation.

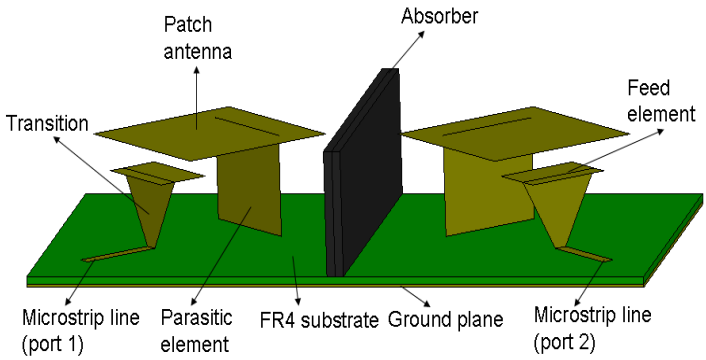

Figure 1. The simulation view of the whole structure.

Besides, the parasitic elements are used to achieve a better return loss within a wider bandwidth where the results with and without these elements are given in the following part. Finally, a rectangular absorber slab (thickness = 6 mm, height = 26 mm) is placed a thin aluminum foil in the middle between two antennas to increase isolation.

In the structure, the positions (height, relative locations) and the dimensions of all elements, the ground plane, are critical in the view of affecting the return loss, coupling and radiation performance. For this purpose, the antenna structure is designed and the dimensions are optimized by using Ansoft HFSSv10 for the best performance within the frequency band 1900–2700 MHz. Initially, the sizes of square patch antennas and ground plane are found as 40 mm × 40 mm and 86 mm × 150 mm, respectively and the center-to-center distance between the patch antennas is 74 mm. The larger dimension of the ground plane is selected as 150 mm after the trade-off between smallest structure size and minimum fields diffracted by the edge of the structures within the desired frequency bandwidth. Then, the height of the patch antennas and position of the feed element are initially assigned and optimized with simulations. However, the structure does not give satisfactory performance especially for the impedance matching. Finally, the position and dimension of the parasitic element are optimized to give the best performance. The relevant dimensions and positions of the final structure are given in Figure 2(a) and (b), which are schematic top and side views of the single element of the system, respectively.

In the phase of the optimization, it is observed that while the parameters w, t, v and u in Figure 2(a) and h_1 in Figure 2(b) are critical tuning parameters in the view of the matching of the antenna,

the parameter u in Figure 2(a) and h_2 in Figure 2(b) are important for isolation performance. Besides, the parameter s (the position of the antenna with respect to feed element) should not be too small that although the small value of this parameter gives good return loss performance. Here, the feed element with transition is a kind of bow-tie antenna where the background of similar structures is given in [12]. This feed element also radiates vertical component, which is important in disturbing the radiation pattern if s is selected too small. By the

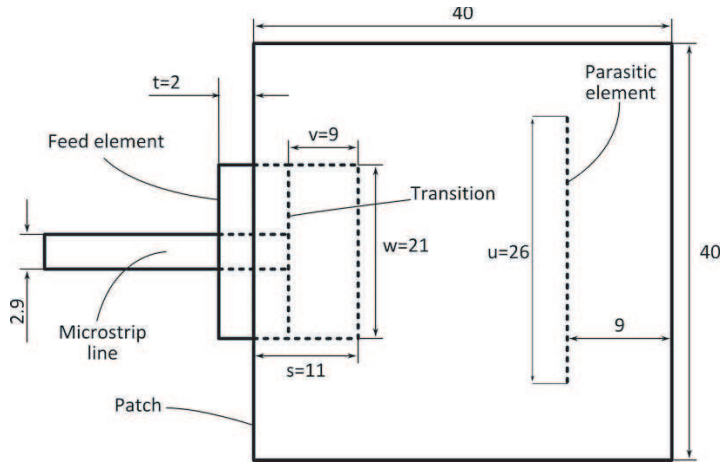

(a)

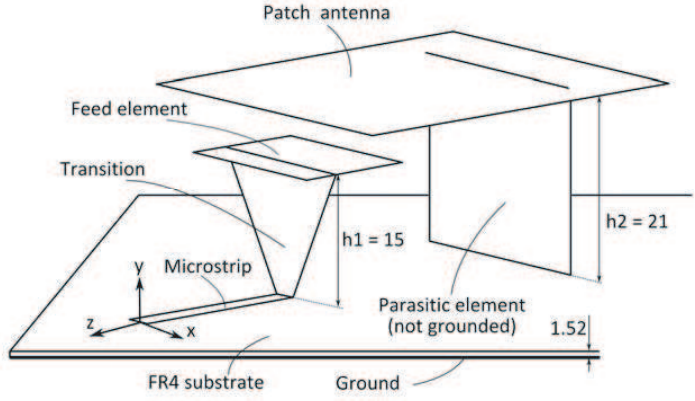

(b)

Figure 2. The schematic view of single element of the structure: (a) Top view, (b) side view (only port 1). The structures are drawn with zero thicknesses and all dimensions are in millimeters.

selection of an appropriate s value, these vertical components are also substantially coupled to the upper patch antenna resulting in a better radiation pattern.

3. THE RESULTS

After the optimization procedure is done, a prototype of the designed structure, whose photograph is shown in Figure 3, is fabricated. As shown in Figure 3, different from simulation view, the prototype is supported with foam-spacers to maintain the mechanical stability of the structure.

After the manufacturing of the prototype, the performance of the structure is measured and compared with the simulation results. In the phase of measurement results, while the return loss and mutual coupling (isolation) are measured with HP8720D vector network analyzer, the radiation pattern and gain performance are obtained in an anechoic chamber. Initially, the input return loss of the port 1 (+45 degrees) of the antenna are obtained for both measurement and simulation where similar results are obtained for port 2 (−45 degrees). For the simplicity, S_{11} parameters are given in Figure 4 for a wider frequency range, 1 GHz–5 GHz, to understand the antenna performance. For the designed frequency bandwidth (1900–2700 MHz), the return loss, which is defined as the negative of the values in Figure 4, is higher than 15 dB, which can be considered as an important advantage of the structure. Besides, the given structure has better results especially for 2100–2700 MHz frequency band covering WLAN band (2400–2500 MHz) and UMTS II band (2500–2700 MHz) that the return loss is above 20 dB in this band. In order to show the effect of parasitic element on enhancing bandwidth, the simulation return loss result without parasitic element is also given in Figure 4 (dashed curve) that the return loss is above 12 dB and can not reach 20 dB within the frequency band for this case. This fact can be explained in

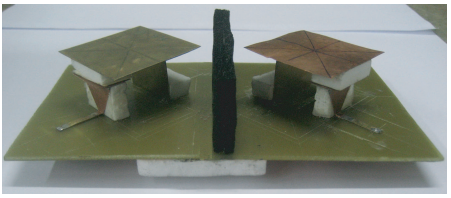

Figure 3. The prototype of the patch antenna system. Two SMA connectors below substrate are bottom-mounted to the microstrip lines.

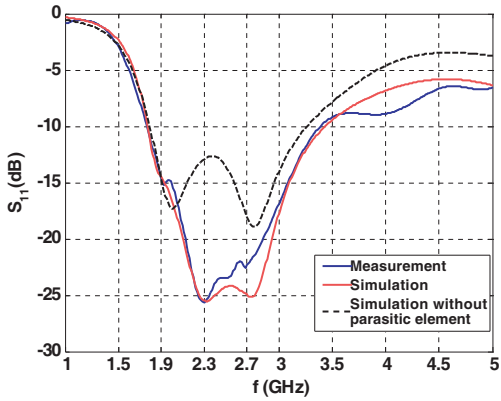

Figure 4. The measured and simulated S_{11} parameters of the proposed structure for 1 GHz–5 GHz band.

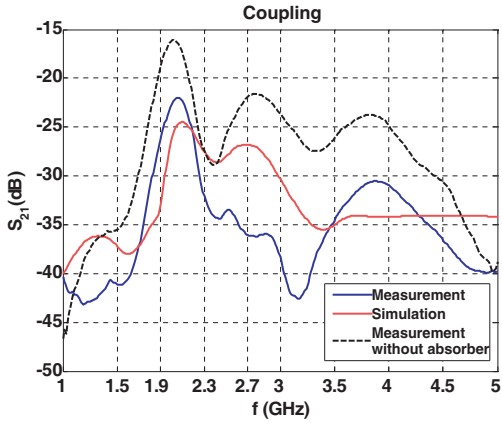

Figure 5. The measured and simulated isolation results of the proposed structure for 1 GHz–5 GHz band.

a way that when the return loss results are examined, the structure shows a band-pass filter characteristics in space and this additional parasitic element acts as series connected inductance and capacitance shunted to ground, and increases the order of this filter by supplying additional tunable parameters to improve the return loss performance.

The isolation (coupling between two patch antennas) performance of the structure belonging to measurement and simulation are obtained and shown in Figure 5 that the isolation is better than 20 dB for both measurement and simulation throughout 1900–2700 MHz frequency

band. When the results in Figure 5 are observed, it can be shown that the coupling has its highest value at about 2 GHz. This fact can be explained that the larger dimension of the ground plane is 150 mm, which corresponds to one wavelength at 2 GHz. Therefore, the surface waves are more effective in this frequency causing the important increase in coupling. Here, in order to demonstrate the effect of the absorber slab, the isolation performance result without absorber slab is also given in Figure 5 (dashed curve) that the absorber slab improves the isolation minimum 5 dB within the designed band. Although the absorber reduces the coupling effect between two ports, it absorbs some portion of the radiated power and reduces the gain. Therefore, the gain of the antenna without absorber should be observed, which is mentioned in the following part. If the degradation in gain is comparably small, adding the absorber between two antennas is important to reduce the coupling.

The radiation and gain characteristics of the proposed structure for the operating frequency bandwidth (1900–2700 MHz) are also investigated. Initially, for the center frequency of bandwidth, 2300 MHz, principal E-plane (yz-plane in Figure 2(b)) and H-plane (xy-plane in Figure 2(b)) patterns for port 1 are given in Figure 6(a) and Figure 6(b), respectively for both measurement and simulation.

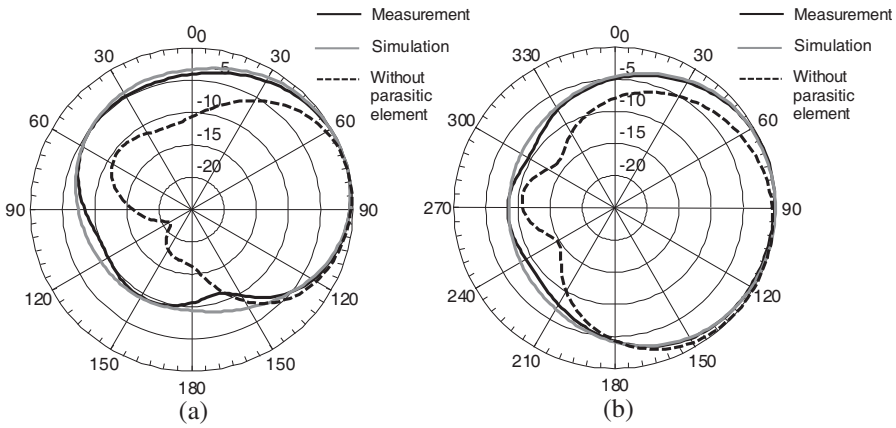

Figure 6. The measured and simulated radiation patterns of the proposed antenna and the patterns of the antenna without parasitic element at the frequency 2300 MHz for the principal planes: (a) E-plane where left and right sides of the patterns correspond to back lobe and main lobe parts, respectively, (yz-plane in Figure 2(b)), (b) H-plane (xy-plane in Figure 2(b)).

According to the results for this sample frequency, the simulation results are similar to measurement results for both planes. In addition to these results, in order to observe the influence of parasitic element on the radiation patterns, the radiation patterns of the antenna without the parasitic element are given in the same figure for both planes of the same frequency. As shown in these patterns, nonexistence of the parasitic element reduces the beamwidth and uniformity in both principal planes and increases asymmetry in E-plane. Therefore, the parasitic element is critical to improve the radiation patterns in addition to improving the impedance matching.

In order to observe the variation of the radiation characteristics with respect to different frequencies, the principal plane patterns are given in Figure 7 for the frequencies 1900 MHz, 2300 MHz and 2700 MHz. From these figures, while H-plane patterns are almost symmetric and uniform within the frequency bandwidth as desired in indoor applications, E-plane patterns show almost uniform patterns for relatively lower frequencies. E-plane patterns show asymmetry with respect to z-axis due to the undesired radiation from microstrip line and feed element, which is also usually seen in the patch antennas having edge microstrip line fed. As mentioned in Section 2, the selection of small s values increase these undesired radiations from feed element and make asymmetry of the radiation patterns larger. For these patterns, the 3-dB beamwidth values corresponding to 1900, 2300

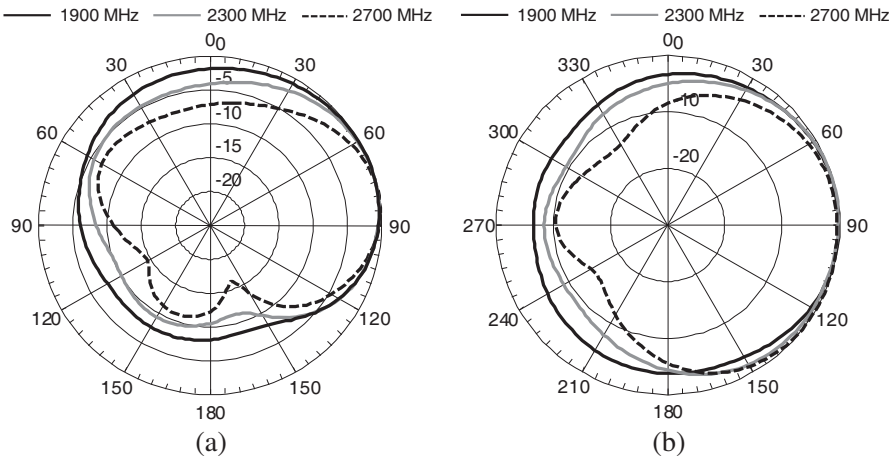

Figure 7. The radiation patterns of the proposed antenna at the frequencies 1900, 2300 and 2700 MHz for the principal planes: (a) E-plane, (b) H-plane.

and 2700 MHz are evaluated respectively as 156, 101 and 66 degrees for E-plane and 144, 146 and 125 degrees for H-plane. When the beamwidth values are searched, the beamwidth values are in the range of 66–156 degrees for E-plane and 125–160 degrees for H-plane, which are sufficiently wide angles for indoor applications.

The gain pattern of the antenna is also obtained throughout the frequency bandwidth, which is given in Figure 8 that the gain values are evaluated between 2.5 dBi and 6.1 dBi. Besides, in order to observe

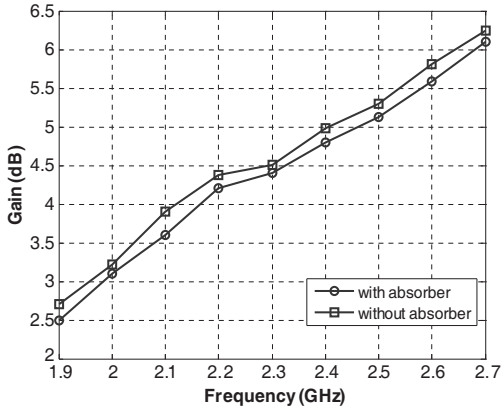

Figure 8. The gain values of the proposed antenna with and without absorber throughout the frequency bandwidth.

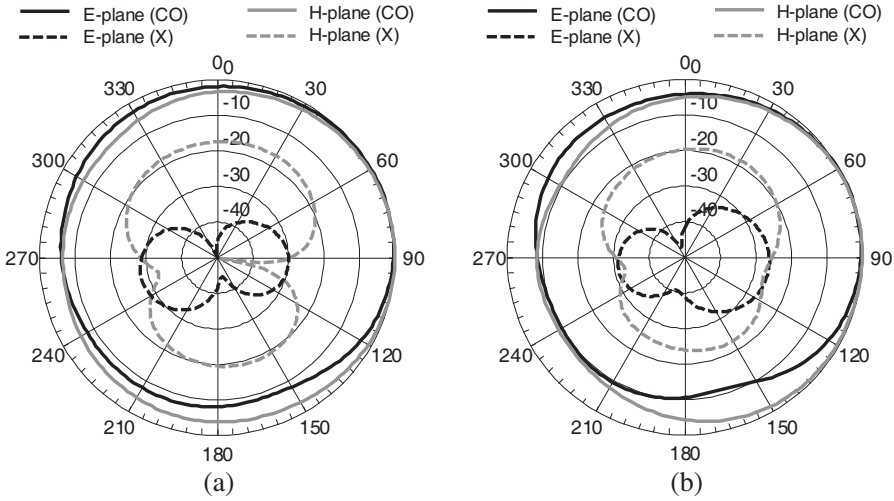

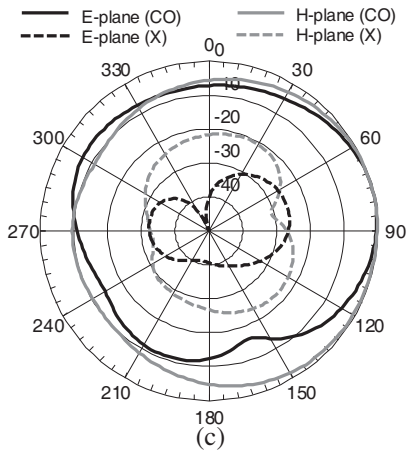

Figure 9. The co-polar and cross-polar radiation patterns of the proposed antenna at the frequencies (a) 1900 MHz (cross polar discrimination (XPD) $>$ 30 dB at 90 degrees), (b) 2300 MHz (XPD $>$ 27 dB at 90 degrees), (c) 2700 MHz (XPD $>$ 26 dB at 90 degrees).

the degradation in gain due to absorber as described before, the gain of the antenna without the absorber is also given in Figure 8. When two results are compared, the gain degradation is at most 0.3 dB making the usage of absorber reasonable to increase the isolation between two ports.

The cross-polarization characteristics (X-pol) of the antenna is also investigated where cross-polarization patterns along with co-polarization patterns (CO-pol) are given in Figure 9 for the same frequencies in Figure 7 that the cross-polar level is found to be at least 25 dB less than co-polar level (cross polar discrimination (XPD) $>$ 25 dB) at the broadside (90 degrees) throughout designed frequency band, which is sufficient for the indoor applications [2]. As a result, the proposed structure is suitable for indoor mobile communication applications when performance results of return loss, isolation, gain and radiation characteristics are considered.

4. CONCLUSION

In this paper, a wide-band dual-polarized antenna structure with a special feed configuration is proposed. The structure is able to operate within the frequency bandwidth 1900–2700 MHz, which covers WLAN, UMTS and extends UMTS bands. The structure is initially designed and optimized; afterwards a prototype of the design is manufactured. The port characteristics (return loss, isolation) and

radiation characteristics (pattern, gain) are tested. From the results, it is concluded from the measurements that the structure has satisfactory performance results supported with simulations. Therefore, the proposed antenna can be used for indoor mobile communication applications.

REFERENCES

1. Serra, A. A., P. Nepa, G. Manara, G. Tribellini, and S. Cioci, "A wide-band dual-polarized stacked antenna," *IEEE Antennas and Wireless Propag. Lett.*, Vol. 6, 141–143, 2007.
2. Chen, Z. N. and K.-M. Luk, *Antennas for Base Stations in Wireless Communications*, McGraw-Hill, New York, 2009.
3. Huang, Y. H., J. Ma, S. G. Zhou, and Q. Z. Liu, "Compact wideband inverted cone combined spherical segment antenna," *Journal of Electromagnetic Waves and Applications*, Vol. 23, No. 7, 935–940, 2009.
4. Song, Y., Y.-C. Jiao, G. Zhao, and F.-S. Zhang, "Multiband CPW-FED triangle-shaped monopole antenna for wireless applications," *Progress In Electromagnetics Research*, PIER 70, 329–336, 2007.
5. Mahatthanajatuphat, C., S. Saleekaw, and P. Akkaraekthalin, "A rhombic patch monopole antenna with modified minkowski fractal geometry for UMTS, WLAN, and mobile Wimax application," *Progress In Electromagnetics Research*, PIER 89, 57–74, 2009.
6. Wu, Y.-J., B.-H. Sun, J.-F. Li, and Q.-Z. Liu, "Triple-band omni-directional antenna for WLAN application," *Progress In Electromagnetics Research*, PIER 76, 477–484, 2007.
7. Vaughan, R. G., et al., "Antenna diversity in mobile communications," *IEEE Trans. on Veh. Tech.*, Vol. 36, 149–172, 1987.
8. Su, D., D. Fu, T. N. C. Wang, and H. Yang, "Broadband polarization diversity base station antenna for 3G communication system," *Journal of Electromagnetic Waves and Applications*, Vol. 22, No. 4, 493–500, 2008.
9. Wong, K.-L., F.-S. Chang, and T.-W. Chiou, "Low-cost broadband circularly polarized probe-fed patch antenna for WLAN base station," *IEEE Int. Symposium on Antennas & Propag.*, Vol. 2, 526–529, San Antonio, Texas, USA, June 2002.
10. Kashani, H. F., M. Shahpari, and H. Ameri, "Dual band dual polarized antenna with high efficiency for base transceiver stations," *Journal of Electromagnetic Waves and Applications*, Vol. 22, No. 10, 1371–1379, 2008.

11. Eldek, A. A., A. Z. Elsherbeni, and C. E. Smith, "Square slot antenna for dual wideband wireless communication systems," *Journal of Electromagnetic Waves and Applications*, Vol. 19, No. 12, 1571–1581, 2005.
12. Herscovici, N., "New considerations in the design of microstrip antennas," *IEEE Trans. Ant. Propag.*, Vol. 46, 807–812, 1998.